photonics

MDPI

Article

Analysis of Copper and Lead in Aerosols with Laser-Induced Breakdown Spectroscopy

Daniel Diaz *, Alejandra Carreon and David W. Hahn

Department of Aerospace and Mechanical Engineering, University of Arizona, Tucson, AZ 85721, USA
* Correspondence: dhdiazo@arizona.edu

Abstract: Laser-induced breakdown spectroscopy (LIBS) was applied to the analysis of aerosolized Cu- and Pb-bearing particles generated from aqueous solutions. A nitrogen-driven nebulizer was utilized to aerosolize Cu- and Pb-spiked solutions. The liquid matrix of the aqueous droplets was evaporated before the LIBS analysis, and the remaining gas-phase analyte-rich aerosols were analyzed in a LIBS system that featured a 1064 nm Nd:YAG laser, a Czerny–Turner spectrometer, and an ICCD camera. The Cu and Pb concentrations in the aerosol streams were 0.26–1.29 ppm and 0.40–1.19 ppm, respectively. Laser diffraction and the particle size distributions of the aqueous aerosols were obtained to indirectly demonstrate the evaporation of the liquid matrix. Highly linear calibration curves (R^2 = 0.995 for Cu and R^2 = 0.987 for Pb) and acceptable limits of detection (2 ppb for Cu and 9 ppb for Pb) and quantification (5 ppb and 28 ppb) were obtained. The applications of the presented methodology include the near-real-time and in situ analysis of wastewater and gas-phase aerosols contaminated with heavy metals.

Keywords: laser-induced breakdown spectroscopy; LIBS; lead; copper; wastewater; heavy metals; aerosols

1. Introduction

The detection and quantification of contaminants in the atmosphere, water bodies, wastewater, and potable water are important in the fields of environmental protection, climate, agriculture, ecology, food and water distribution, and public health. The contaminants of interest have multiple origins, but heavy metal contamination usually comes from industrial processes [1–3] and the aging of heavy-metal-bearing pipes and accessories utilized for water transportation [4,5]. Heavy metals such as Cu and Pb are of special interest due to their potentially harmful effects on human health. Pb, for instance, is persistent (slow to break down) and can bioaccumulate (accumulation in a biological organism). Possible effects that range from stomach distress to brain damage can be associated with the heavy metal content in drinking water [4]. Optical spectroscopy techniques such as atomic absorption spectroscopy (AAS), atomic fluorescence spectrometry (AFS), and inductively coupled plasma optical emission spectroscopy (ICP-OES) are typically utilized to monitor heavy metals from various sources [3,6–9]. In AAS and AFS, the sample is first atomized and decomposed into gas phase using plasmas, flames, or electrothermal atomizers. The gaseous sample is then probed by a single-wavelength light source, which is absorbed by the constituent atoms. In AAS, the amount of absorbed light is measured as it is proportional to the analyte's concentration. AFS measures the analyte's characteristic fluorescence emission after excitation by light absorption [6,7]. AAS and AFS can be utilized for analysis of various elements; however, the analysis is typically performed one element at a time, which adds complexity and turnaround time. ICP-OES uses its high-temperature plasma to atomize and ionize a sample fed in aerosol form. The atomic emission of the excited atoms, which is proportional to the analyte concentration, is then measured. Unlike AAS and AFS, ICP-OES is a multi-elemental technique [6,7]. These three techniques are well established

check for updates

Citation: Diaz, D.; Carreon, A.; Hahn, D.W. Analysis of Copper and Lead in Aerosols with Laser-Induced Breakdown Spectroscopy. *Photonics* **2024**, *11*, 1112. https://doi.org/10.3390/photonics11121112

Received: 29 October 2024
Revised: 20 November 2024
Accepted: 23 November 2024
Published: 25 November 2024

Copyright: © 2024 by the authors. Licensee MDPI, Basel, Switzerland. This article is an open access article distributed under the terms and conditions of the Creative Commons Attribution (CC BY) license (https://creativecommons.org/licenses/by/4.0/).

and have excellent analytical figures of merit. In general, they are bulky, time-demanding, and costly; they require sample preparation and concentration calibration and are not suitable for real-time in situ analysis.

Depending on the source, Cu and Pb concentrations in wastewater effluents can vary from tens to thousands of parts per million (ppm), and remediation processes are required before discharge to the environment [8,10,11]. Current remediation processes should reduce the Cu and Pb concentrations to 2 ppm and 10 ppb [12], respectively, before discharge. In the case of potable water, it has been agreed that there is no known safe concentration of a contaminant such as Pb [5]. However, because Cu and Pb contamination of drinking water originates mostly from aging of plumbing materials, government agencies have established reference Cu and Pb concentrations (known as action levels) based on the effectiveness of corrosion treatments of water systems rather than based on maximum contaminant concentrations [5]. The action levels for Cu and Pb are, respectively, 1.3 ppm and 15 ppb [4,5]. Contaminant concentrations that exceed the action levels in more than 10% of tap water samples would trigger the execution, by the public water system, of multiple activities such as lead service line replacement and public education to address the findings [5]. In the case of Pb, lead-free regulations have also been established that prohibit the use of pipes, fittings, solder, and flux that exceed specified Pb concentrations [13].

Laser-induced breakdown spectroscopy (LIBS) is an atomic emission spectroscopy technique that uses a focused laser beam to produce a plasma on a target, which can be solid, liquid, gas, or aerosol. Laser absorption by the targeted material induces heating, melting, vaporization, atomization, and ionization of its constituent elements. As the excited elements decay, they emit characteristic light that can be utilized as a chemical fingerprint. Collection, wavelength dispersion, and detection of the light emitted by the plasma allow qualitative and quantitative elemental analysis [14]. The most well-known advantages of LIBS are its capacity to perform near-real-time analysis of any element with minor or no sample preparation in tabletop, stand-off, and remote configurations. Multiple reports and reviews exist regarding the use of LIBS for the analysis of several analytes in liquid solutions [15–18]. In general, the sampling of liquid targets can be done on the liquid surface [19,20] or inside the liquid [21]; after freezing [20], through the generation of droplets [22], jets [23,24], and aerosols [14,25–27]; and by depositing the solutions onto substrates [16–18]. In addition, the application of LIBS for analysis of heavy metals has been carried out in solids [28], liquids [29], gases [30], and aerosols [31,32].

In particular, the LIBS analysis of Cu and Pb in aqueous solutions has also been reported, and a summary of relevant results for this investigation follows. When possible, all values are reported as mass/mass part per million (ppm) or billion (ppb) for a straightforward comparison among the limits of detection (LOD). Sobral et al. [20] reported the LODs for Cu and Pb when aqueous solutions were analyzed by direct liquid surface sampling and ice surface analysis after freezing the solution. Freezing the solutions provided better LODs than direct liquid surface analysis. The LODs for liquid surface analysis were 9.6 for Cu and 12.5 ppm for Pb, whereas the corresponding values for ice analysis were 2.3 and 1.3 ppm. This methodology requires the use of a freezer and extends the analysis time as the samples need to be converted to ice. Lee et al. [33] reported the analysis of Cu and Pb from aqueous solutions deposited and preconcentrated on filter papers. The aqueous solutions were deposited on a paper and then evaporated in an oven. The LOD of Pb was reported as 2.7 ppm. Further improvement in the LOD (i.e., 75 ppb) values was reported by increasing the amount of solution utilized for preconcentration; however, the evaporation method lasted about 1 h and required amounts of solution of the order of 40 g. Following the same method, Cu emission lines were found in tap water samples with a Cu concentration of 641 ppb. Zhao et al. [34] electrically deposited the metal ions Cu^{2+} and Pb^{2+} dissolved in tap water on a high-purity aluminum rod for LIBS analysis. The LODs for Cu and Pb were, respectively, 0.162 ppb and 0.570 ppb. An improvement of 2 orders of magnitude for the LODs with respect to the direct analysis of aqueous solutions was reported. This methodology requires an electrically driven apparatus for sample deposition, deposition

times of about 20 min, and a high-purity deposition rod that may need replacement due to continuous surface ablation.

Aerosolizing or nebulizing liquid samples is another approach for chemical analysis with LIBS [14,25,26,35]. The analysis of aqueous or other types of aerosols can be realized through direct analysis of the aerosol stream and analysis after deposition of the aerosol particles on substrates [14]. Direct aerosol analysis only requires optical access to the process and can provide real-time results. Indirect analysis may improve the performance due to a preconcentration effect of the analytes; however, spectral interferences may be found, and the collection time on the substrates increases the total analysis time. Aras et al. [35] utilized LIBS to analyze various sub-micron aerosol particles of various elements, including Cu and Pb. The aerosols were produced from aqueous solutions after ultrasonic nebulization, desolvation, and further drying through a membrane filter. The aerosol stream was then sampled with a LIBS system. The LODs for Cu and Pb were, respectively, 1.99 and 13.6 ppm. In order to investigate the effect of the nebulizing gas on the LIBS signals from Cu-containing aerosol particles, Palazzo et al. [36] reported LODs for Cu as 23 ppb in air and 41 ppb in nitrogen. Indirect analysis was reported by Panne et al. [31], who sampled aqueous solutions containing heavy metals such as Cu and Pb deposited on quartz fiber filters. The LODs per unit area for Cu and Pb were, respectively, 0.01 and 0.06 $\mu g/cm^2$.

This research reports a proof-of-concept LIBS analysis of gas-phase aerosols produced from aqueous solutions spiked with Cu and Pb. The approach involves the nebulization of analyte-bearing aqueous solutions followed by a drying step of the water content and LIBS analysis of the remaining analyte-rich solid particles in a N_2 gas stream. Cu- and Pb-spiked water solutions were prepared, nebulized, dried, and then analyzed with LIBS. Laser diffraction was utilized to characterize the nebulized aqueous droplets. Linear calibration curves and acceptable LODs and limits of quantification (LOQ) were obtained through this experimental approach.

2. Materials and Methods

2.1. Aerosol Generator and LIBS System

The experimental setup consisted of two custom-made components: an aerosol generator system and a LIBS system, as depicted in Figure 1 [25,26]. A 15-mL medical nebulizer (McKesson, Irving, TX, USA), which holds a liquid sample, generates a fine mist of submicron to micron-sized particles when a driving gaseous flow enters through the nebulizer inlet. The nebulizer is connected to a stainless-steel tapered cylinder that allows mixing and drying after nebulization of the sample. A N_2 coflow is introduced through a porous plate at the base of the tapered section to evaporate the aqueous aerosol droplets and transport the resulting analyte-rich solid particles to the LIBS chamber [25,26,36,37]. The nebulizer driving flow and coflow were powered by compressed and filtered N_2 gas. The flow rates were kept constant at 5 slpm for the driving flow and 20 slpm for each coflow gas, for a total of 45 slpm running through the system. Flow measurements were adjusted at standard conditions (298.5 K and 101,325 Pa).

The LIBS analysis chamber rests on top of the aerosol generator and has a six-way stainless-steel vacuum cross with 38 mm diameter flanges. To focus the laser beam, a UV-grade 50 mm diameter plano-convex lens with a focal length of 75 mm (L1) was mounted on the horizontal flange that faced the laser system (see Figure 1). Quartz windows and solid stainless-steel covers were fitted on the other horizontal flanges. The vertical top flange was connected to an exhaust system. Neoprene gaskets sealed all flanges airtight. The LIBS system included a Nd:YAG laser (Surelite I-10, Continuum Inc., Santa Clara, CA, USA) delivering 10 ns pulses of 6 mm diameter at a wavelength of 1064 nm. The laser system ran at a repetition rate of 5 Hz with a nominal beam energy of approximately 400 mJ. This beam was split into two beams with a nonpolarizing beamsplitter (angle of incidence: 45 degrees, 50% reflective). The beam splitting is not shown in Figure 1 as it is not relevant for this research. The laser beam utilized in the current LIBS setup had a maximum energy

of 178.9 ± 1.5 mJ per pulse. The second beam was utilized for a different setup. The focused spot diameter for this optical configuration is estimated to be 0.5 mm for an approximated fluence of 9.2 J/cm^2 and irradiance of 9.2 × 10^9 W/cm^2. A high irradiance is desirable when analyzing gases and aerosols to guarantee the production of the laser-induced plasma at each single laser pulse in clean nitrogen (without the presence of aerosol particles). The beam energy was measured with a pyroelectric energy meter (Ophir, Andover, MA, USA). The beam energy was maintained constant across all the experiments. However, the beam energy of the Nd:YAG laser utilized in this research can be varied by adjusting the q-switch delay time (i.e., time between the command to fire the flashlamp and the command to fire the Pockels cells) and/or adapting a combination of a half-wave plate and a polarizer in the beam path. The former method does not require any extra components but induces a change in the pulse duration. The latter method requires extra optical components but allows for a continuous variation of energy by rotating the half-wave plate.

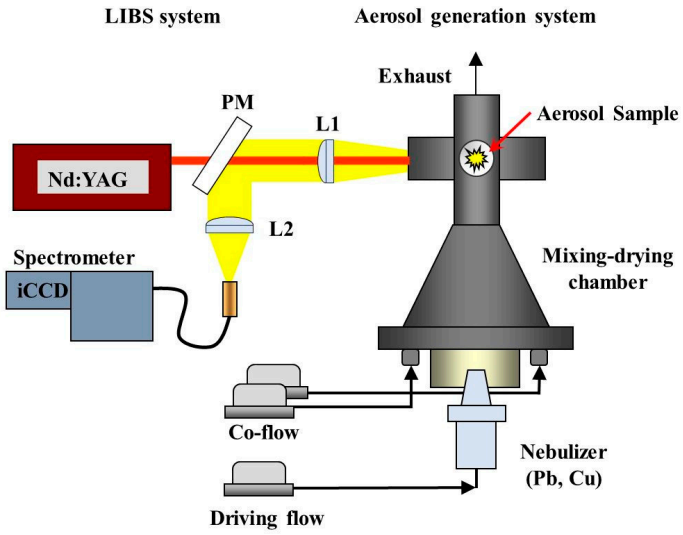


Figure 1. Scheme of LIBS and aerosol generation systems. L1 and L2: plano-convex lenses; PM: pierced mirror.

The laser was aligned and focused on the geometrical center of the analysis chamber. The light emitted by the plasma was captured in backscattered mode and collimated by the lens L1. The collimated light was reflected 45 degrees by a pierced mirror (Al-enhanced coating) and then focused onto a fiber optic (2 m length, 200 μm diameter, 19-fiber bundle) by a second UV-grade 50 mm diameter plano-convex lens with a focal length of 75 mm (L2). The plasma light was resolved by a Czerny–Turner spectrometer (Teledyne Princeton Instruments, NJ, USA) with a focal length of 0.5 m (1800 grooves/mm grating) and registered by an ICCD detector (256 × 1024 pixels). Spectra of approximately 25 nm wide were obtained with a spectral resolution of 0.10 nm.

2.2. Samples

The aqueous solutions were created by spiking distilled water with various amounts of Cu (10,000 μg/mL in 5% HNO) and Pb (10,000 μg/mL in 5% HNO_3) standard solutions (Spex CertPrep). The Cu and Pb aqueous concentrations ranged, respectively, from 1000 to 200 μg/mL and 3004 to 1001 μg/mL. These concentration ranges represent highly contaminated wastewater samples that would require the application of a remediation process for safe use. In the nebulization processes, the aqueous solutions are diluted by the nitrogen gas, thus creating concentrations from 0.26 to 1.29 ppm for Cu and 0.40 to 1.19 ppm for Pb. Table 1 presents the analyte concentrations of the stock solutions (columns 1 and 2) and the concentrations in the aerosol stream (columns 3 and 4). Tap and distilled water were utilized as blank samples and measured under identical conditions to the

analyte-bearing samples. The tap water samples were taken from the laboratory facilities. Tap water was utilized as a blank because it was expected that no detectable amounts of Cu or Pb were present in the laboratory facilities. This was then confirmed through LIBS analysis as no observable emission lines of Cu and/or Pb were found in the LIBS spectra. Furthermore, the use of tap water allowed for the investigation of the potential presence of other emission lines that would create spectral interference with the Cu and Pb emission lines. No significant interfering emission lines were found except the emission line at ~406 nm, which will be discussed in Section 3.2. Each sample, including the blanks, was analyzed 3 times. The measurement time was 6.7 min.

Table 1. Analyte concentrations in the aqueous solution and the gas-phase aerosol stream.

Solution (μg/mL)		Aerosol (ppm)	
Cu	**Pb**	**Cu**	**Pb**
1000	3004	1.29	1.19
800	2504	1.03	0.99
600	2003	0.77	0.79
400	1502	0.51	0.59
200	1001	0.26	0.40

2.3. Spectra Analsys

Each sample was measured for 6.7 min at a laser repetition rate of 5 Hz for a total of 2000 single-shot spectra. Single-shot spectra were ensemble averaged, and the analyte net intensity was calculated as the peak intensity minus the background intensity. The net intensity calculated in this manner was utilized to build the Cu and Pb calibration curves. Signal normalization was not required. Due to the significant background noise observed, a single-pixel approach for the peak and background intensity was employed with satisfactory results. The emission line Cu I 324.8 nm was used to detect copper. The delay and gate times that provided the best signal-to-noise ratio for this Cu line were 11 and 25 μs, respectively. The emission line Pb I 405.8 nm was used to detect lead. The delay and gate times that resulted in the best signal-to-noise ratio for this Pb line were 13 and 25 μs, respectively. Simultaneous detection of Cu and Pb is desirable; however, it was not realized due to the narrow spectral bandwidth provided by the spectrometer configuration (i.e., ~25 nm). The limits of detection (LOD) and quantification (LOQ) were calculated as $3 \times SD_b/m$ and $10 \times SD_b/m$ [38], respectively. Where SD_b is the standard deviation of the blank sample (or background), m is the slope of the calibration curve, and the factor 3 accounts for a 99.9 confidence level [38].

3. Results and Discussion

3.1. Characterization of the Aerosol Generation System

In general, a pneumatic jet nebulizer converts a liquid sample into an aerosol stream with particle sizes varying from the submicron to micron size range [39,40]. The nebulizer is driven by a compressed gas that expands after flowing through a narrow orifice. The expanding gas jet creates a region of negative pressure that draws liquid up a feeder tube. The lower end of the feeder tube is immersed in the sample reservoir, whereas the upper end is near the orifice. The liquid enters the gas jet and impacts a plate where the liquid is broken into droplets of different sizes. Larger droplets fall back into the liquid, whereas the smaller particles leave the nebulizer [40].

To provide a known and controlled amount of aerosol particles, the aerosol generation system requires calibration between the nebulizer output rate and the nebulizer driving gas flow [25–27]. Knowledge of the nebulizer output rate, the analyte concentration of the solution deposited in the nebulizer, and the coflow rate allows the calculation of the analyte mass concentration within the LIBS sampling chamber [25–27]. The calibration procedure was performed by measuring the total mass of the nebulizer (nebulizer plus liquid sample)

before and after nebulization for periods of 10, 20, and 30 min at driving flow rates between 1.5 and 5.0 slpm. A linear calibration curve (R^2 = 0.997) between the nebulizer output rate and the nebulizer driving gas flow was obtained. The overall relative standard deviation (RSD%) of all measurements was 1.7%. The high value of the coefficient of determination and the low RSD magnitude demonstrated the ability of the nebulizer to provide uniform amounts of aerosol streams over the tested operational range. The calibration equation was utilized to calculate the analyte mass concentration in the aerosol stream within the LIBS sampling chamber. The mass concentrations obtained were presented in Table 1.

Particle size characterization of the aerosols produced by the nebulizer only and the aerosol generator was performed with a laser diffraction particle analyzer (HeNe laser, 632.8 nm, 10 mm diameter). Samples of distilled water were deposited into the nebulizer, and laser diffraction measurements were performed at the nebulizer outlet. This was conducted to characterize the aqueous aerosols directly from the nebulizer (without the aerosol generation system). A new sample was deposited into the nebulizer, installed in the aerosol generation system, and laser diffraction measurements were performed at the exit of the generator. In all cases, the nebulizer was always driven with N_2 at a rate of 5 slpm. In the case of the generator, measurements were performed with the coflow gas off and then on at a total rate of 40 slpm. Figure 2 shows the water particle size distribution (PSD) obtained directly from the nebulizer (dots) and at the outlet of the aerosol generator (squares) with no coflow gas. The modal diameter (most probable particle size) for both distributions was 6.81 μm; that is, both distributions have the same peak diameter. The 50% percentile diameter for the nebulizer alone was 6.20 μm, and when the nebulizer was installed into the generator, this percentile diameter was 6.30 μm. The volume concentration (area under the curve) did not significantly vary or follow any specific trend in repeated measurements. The volume concentration, however, increased towards smaller particles (in the range between ~3.70 and 10.80 μm) for the aerosol produced through the generator (squares in Figure 2). This indicates a size reduction due to evaporation or breakage of larger particles into smaller particles as the aerosol travels along the generator. Because the volume concentration remained unchanged, the former argument seems most reasonable. It should also be considered that the nebulizer was affixed directly within the measuring region of the particle analyzer (i.e., between the laser and the detectors of scattered light), and the aerosols exiting the nebulizer were measured at the exact outlet of the nebulizer. Due to its size, the generator could not be located within the measurement region of the particle analyzer; instead, an s-shaped plastic hose (25 mm diameter, 300 mm length) was utilized to transport the aerosols from the generator to the particle analyzer. The extra travel length (i.e., generator length plus hose) and hose shape may be responsible for the slight particle size reduction due to mechanical impact with surfaces. The trace amounts of analytes added to the water samples did not change the general particle size distributions.

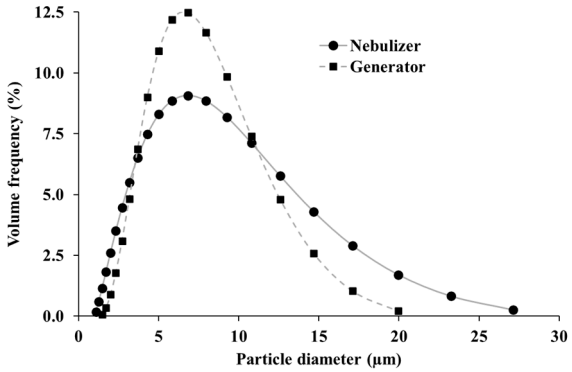


Figure 2. Particle size distribution of water aerosols obtained at the outlet of the nebulizer (dots, continuous line) and at the outlet of the generator (squares, dashed line).

Laser diffraction measurement of aerosolized analytical samples (i.e., distilled water spiked with analytes as per Table 1) when the total N_2 flow was applied (45 slpm) to the aerosol generator system showed no significant scattering signal, and no significant difference in the scattered signals was found between those results and laser diffraction measurements of static room air and a nitrogen flow at a rate of 45 slpm. The absence of scattering signals indirectly indicates that the larger water droplets were evaporated, and, because LIBS signals were detected in the aerosol stream, solid analyte-rich particles remained. Direct PSD measurements of the remaining solid particles were not possible because of the particle analyzer resolution (~0.1–0.5 μm). This was expected, as the modal particle sizes of particles generated in a similar aerosol generator (and measured with transmission electron microscopy) were reported to be in the range between 9.5 and 50 nm for iron oxide and titanium oxide, respectively [25].

Considering a binary mixture of water vapor in air [25], the time for droplet evaporation can be estimated through the D^2 law [25,41]. The particle lifetime was calculated for the modal particle size (i.e., 6.81 μm) and the largest particle size (i.e., 27.1 μm) obtained from the PSD of the nebulized distilled water. The respective lifetimes were 0.013 and 0.21 s, whereas the average residence time for an aerosol particle traveling along the aerosol generator is 0.60 s. The evaporation parameters utilized to calculate the particle lifetime were reported by Hahn et al. [25]. The fact that the residence time was estimated to be 3 times the lifetime for the largest aqueous particle lifetime supports the assumption that the aqueous droplets were fully evaporated.

The drying of the aqueous droplets is desirable for the improvement in LIBS analytical performance due to three main reasons: (a) reduction in matrix effects and enhancement of stoichiometric ablation due to the absence of the liquid and quenching matrix; (b) a cleaner laser beam path for delivery of beam energy into the focal point and reduction in prebreakdown effects due to elimination of large water droplets; and (c) reduction in optics contamination. As discussed in the next section, the elimination of the liquid matrix in the drying process allowed the use of straightforward and rapid spectral processing (i.e., univariate, no normalization, single-pixel net intensity) and the obtention of linear trends within relatively narrow confidence bands and acceptable LOD, LOQs, and RSD values. The approach utilized in this research differs from the more conventional methods for analysis of liquid samples, namely, surface analysis and deposition on substrates.

3.2. Calibration and Detection Limits

Linear calibrations for the analytes Cu and Pb were obtained using the LIBS net intensity, as shown in Figure 3b,d. The values of the coefficients of determination (R^2) were 0.995 for Cu and 0.987 for Pb. The error bars in Figure 3b,d represent one standard deviation. The linear trend for both analytes is clear in both the spectra (Figure 3a for Cu and Figure 3b for Pb) and calibration plots. The 95% confidence bands, shown in dashed lines, showed a narrower dispersion of Cu compared to Pb. This may be attributed to the stronger Cu emission intensity. The emission Cu I 424.8 nm involves the ground state [42] and, therefore, presents a higher relative intensity. The average uncertainties of the concentration measurements determined for a 95% confidence level were 7% for Cu and 13% for Pb. Although these figures are higher compared with conventional analytical techniques (e.g., AAS, ICP-OES), they are reasonable for LIBS analysis of aerosols [32]. The lower than desirable accuracy of LIBS is well known; however, this apparent limitation is compensated for by the well-known advantages of LIBS of inexpensive near-real-time analysis and in situ capabilities.

The emission line around 406 nm and adjacent to the Pb line (labeled as interference) did not hinder the quantification of the Pb line intensity for the concentration range shown in Table 1; however, it became relevant for lower concentrations of Pb. Although the source of this line is not known with certainty, the fact that it appeared in all samples and blanks with a relatively constant intensity may indicate that it belongs to hydrogen, nitrogen, or oxygen. H or N emission lines were found in the range between 405.5 and 406.5 nm;

however, several O II emission lines are visible in this range [42]. Blank samples did not show any analyte emission line in the spectral ranges observed, confirming their utility as blanks.

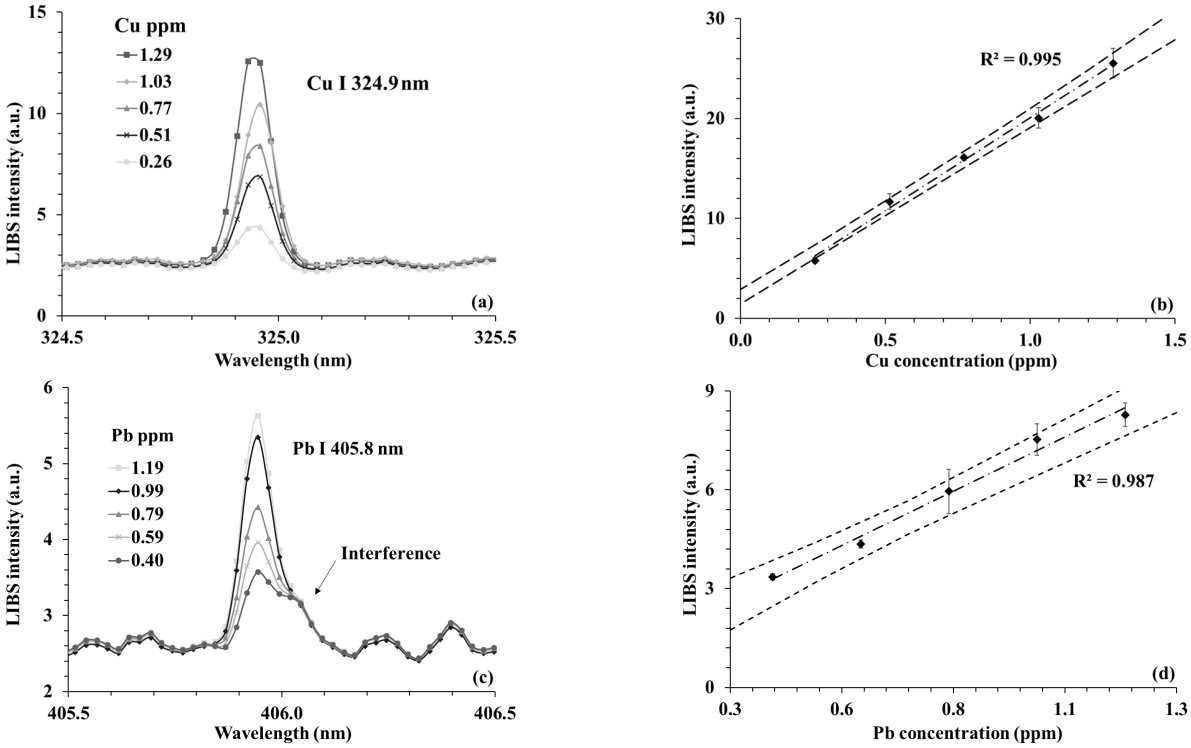


Figure 3. Spectral and calibration curves. (**a**) Cu I emission line for various concentrations; (**b**) Cu calibration curve (dashed dot) and confidence bands (dashed line); (**c**) Pb I emission line for various concentrations; (**d**) Pb calibration curve (dashed dot) and confidence bands (dashed line). Error bars represent one standard deviation.

An aerosol sample with Pb concentration of 0.20 ppm (Pb concentration of 500 µg/mL in solution) was analyzed in similar conditions, and, although the Pb emission line was still visible, the constant intensity interference overlapped significantly with the Pb analyte line. At these Pb concentration levels, the overlapping can be solved readily by deconvoluting the emission profiles; however, lower concentrations may result in a complete obstruction of the analyte line and additional uncertainty to the measurements. Current work is being done regarding lower concentrations and the application of conditional analysis to improve the LIBS sensitivity when analyzing extremely low analyte concentrations [26,32].

The minimum Cu concentration sampled with LIBS was 0.26 ppm, and the LOD and LOQ were, respectively, 2 and 5 ppb. For Pb, the minimum concentration sampled was 0.40 ppm, and the LOD and LOQ were, respectively, 9 and 28 ppb. The LOD and LOQ values were approximated to the nearest integer. In the context of analyzing highly contaminated wastewater that needs to be treated before discharge to the environment, the LIBS performance and the obtained LOD values are promising.

The LOD values obtained in this work were below or on the same order of magnitude as those reported in previous publications [20,31,33,35,36]. Zhao et al. [34] reported lower LODs than in the current work (0.162 ppb for Cu and 0.570 ppb for Pb), which can be attributed to the preconcentration effect created by the electrical deposition. However, a more complex setup and time-consuming methodology were required. In contrast, the methodology presented herein can be considered near real time (5 to 10 min), and, although the current setup is of tabletop size, the LIBS system can be readily miniaturized. The repeatability of the measurements was estimated by calculating the RSD% of three replicate measurements. The RSD% values of the Cu and Pb measurements were 4.8% and

5.5%, respectively. These reasonably low RSD values show an acceptable repeatability for relatively low sampling times.

The current experimental setup can be utilized to monitor any other heavy metals as long as their concentration is higher than the limit of detection of the LIBS system and the analytes have emission lines within the observable spectral range, which is between ~250 and ~900 nm for the current setup. Notice, however, that the spectral window of observation is about 25 nm for a single measurement.

Although the obtained LODs and LOQs are reasonable, some of the strategies that can be utilized to improve the sensitivity of a LIBS system for aerosol analysis are (a) increase in the beam energy to create a larger and higher temperature plasma that would excite a larger amount of sample and therefore lead to a higher number of excited species [43]; (b) selection of emission lines of higher intensity, free of interferences, and/or reducing the background emission intensity and noise of the spectra around the analyte's emission lines [44–46]; (c) aerosolization with a gas such as argon, which is known to produce higher-temperature plasmas [47]; and (d) use of conditional analysis by selectively distinguish between spectra with emission lines from those without emission lines [14,26,32].

The calculated LODs were below the Cu and Pb action levels for drinking water; however, the initial stock solutions (columns 1 and 2 in Table 1) contain considerably high concentrations of those heavy metals. The methodology presented in this work can be applied to aqueous samples with lower heavy metal concentrations by reducing the dilution factor during the aerosol generation. The reduction in the dilution factor can be realized by decreasing the coflow rate. For example, by reducing the coflow rate by a factor of 10, the concentration of the original stock solutions can be decreased by a factor of 5. The residence time of the aqueous aerosol particles increases by a factor of 5, providing even more time for drying of the water content. Further reductions in dilution factor can be achieved by modifying the aerosol generation system (e.g., increasing length).

Because the LIBS analysis is performed in a gas-phase aerosol (i.e., aerosol where the dispersing medium is a gas), the results of this work can be extrapolated to the analysis of heavy metals in gaseous streams from industrial processes such as combustion and atmospheric particulate matter.

4. Conclusions

This investigation aimed to address the detection of heavy metals Cu and Pb in gas-phase aerosols generated from aqueous samples. The successful application of LIBS for detection and quantification of Cu- and Pb-bearing particles coming from aqueous solutions was demonstrated by the obtention of linear calibration curves and reasonable limits of detection and quantification. Samples of Cu- and Pb-spiked water were created and analyzed with LIBS. The aqueous samples were first aerosolized and dried, and the resulting analyte-bearing particles were sampled with a LIBS probe. The results showed that LIBS detection of gas-phase Cu and Pb aerosols is possible at concentration levels of 2 and 9 ppb, respectively. Quantification would require concentration levels of 5 ppb for Cu and 28 ppb for Pb. Compared to previous publications, in addition to providing lower LOD and LOQ values, the LIBS system utilized in this work required a relatively simple auxiliary device for the generation of the aerosol particles that is portable and could also be reduced in size. In addition, the improvements in the analytical performance obtained by analyzing aerosols rather than liquid samples were demonstrated. It is considered that the evaporation of the water content improved the LIBS analytical performance by reducing matrix effects and improving stoichiometric ablation. Based on the experimental setup, the experimental methodology, and the obtained analytical figures, this research demonstrates that the well-known advantages of LIBS for rapid aerosol analysis can be utilized to develop a portable sensor for analysis of multiple heavy-metal-bearing samples, including wastewater, treated water (after remediation processes), and drinking water, at several locations within processes, transport, and water distribution systems. Furthermore, because the LIBS analysis was performed in a gas-phase aerosol, this work can be extrapolated to

the analysis of heavy metals in gaseous streams and effluents from industrial processes. Future work includes the analysis of actual contaminated water samples from municipal and industrial water systems as well as flue gases from industrial processes.

Author Contributions: Conceptualization, D.D. and D.W.H.; methodology, A.C. and D.D.; software, A.C. and D.D.; validation, A.C. and D.D.; formal analysis, A.C. and D.D.; investigation, A.C. and D.D.; resources, D.D.; data curation, D.D.; writing—original draft preparation, A.C. and D.D.; writing—review and editing, D.D.; visualization, D.D.; supervision, D.D. and D.W.H.; project administration, D.D. and D.W.H.; funding acquisition, D.D. and D.W.H. All authors have read and agreed to the published version of the manuscript.

Funding: This research received no external funding.

Data Availability Statement: The raw data obtained in this research will be made available by the authors on request.

Acknowledgments: The authors acknowledge partial support from Provost Investment Funds 2022, University of Arizona (Tucson, AZ, USA).

Conflicts of Interest: The authors declare no conflicts of interest.

References

1. Sharma, S.; Bhattacharya, A. Drinking water contamination and treatment techniques. *Appl. Water Sci.* **2017**, *7*, 1043–1067. [CrossRef]
2. Tchounwou, P.B.; Yedjou, C.G.; Patlolla, A.K.; Sutton, D.J. Heavy metal toxicity and the environment. In *Molecular, Clinical and Environmental Toxicology*; Luch, A., Ed.; Springer: Basel, Switzerland, 2012; pp. 133–164. [CrossRef]
3. Popoola, L.T.; Adebanjo, S.A.; Adeoye, B.K. Assessment of atmospheric particulate matter and heavy metals: A critical review. *Int. J. Environ. Sci. Technol.* **2017**, *15*, 935–948. [CrossRef]
4. United States Environmental Protection Agency, Lead and Copper Rule. 2023. Available online: https://www.epa.gov/dwreginfo/lead-and-copper-rule (accessed on 17 September 2024).
5. United States Environmental Protection Agency, Basic Information About Lead in Drinking Water. 2024. Available online: https://www.epa.gov/ground-water-and-drinking-water/basic-information-about-lead-drinking-water (accessed on 17 September 2024).
6. Llaver, M.; Oviedo, M.N.; Quintas, P.Y.; Wuilloud, R.G. Analytical Methods for the Determination of Heavy Metals in Water. In *Remediation of Heavy Metals; Environmental Chemistry for a Sustainable World*; Inamuddin, Ahamed, M.I., Lichtfouse, E., Altalhi, T., Eds.; Springer: Cham, Switzerland, 2021; pp. 1–37.
7. Ingle, J.D.; Crouch, S.R. *Spectrochemical Analysis*; Prentice-Hall Inc.: Englewwod Cliffs, NJ, USA, 1988.
8. Punia, P.; Bharti, M.K.; Dhar, R.; Thakur, P.; Thakur, A. Recent Advances in Detection and Removal of Heavy Metals from Contaminated Water. *ChemBioEng Rev.* **2022**, *9*, 351–369. [CrossRef]
9. Jin, M.; Yuan, H.; Liu, B.; Peng, J.; Xu, L.; Yang, D. Review of the distribution and detection methods of heavy metals in the environment. *Anal. Methods* **2020**, *12*, 5747–5766. [CrossRef] [PubMed]
10. Liu, Y.; Wang, H.; Cui, Y.; Chen, N. Removal of Copper Ions from Wastewater: A Review. *Int. J. Environ. Res. Public Health* **2023**, *20*, 3885. [CrossRef]
11. Ucun, H.; Bayhana, Y.K.; Kaya, Y.; Cakici, A.; Algur, O.F. Biosorption of lead (II) from aqueous solution by cone biomass of Pinus sylvestris. *Desalination* **2003**, *154*, 233–238. [CrossRef]
12. World Health Organization. *Guidelines for Drinking-Water Quality*, 4th ed.; World Health Organization: Geneva, Switzerland, 2022.
13. United States Environmental Protection Agency, Use of Lead Free Pipes, Fittings, Fixtures, Solder, and Flux for Drinking Water. 2024. Available online: https://www.epa.gov/sdwa/use-lead-free-pipes-fittings-fixtures-solder-and-flux-drinking-water (accessed on 17 September 2024).
14. Diaz, D.; Hahn, D.W.; Panne, U. LIBS for aerosol analysis. In *Laser-Induced Breakdown Spectroscopy*, 2nd ed.; Singh, J.P., Thakur, S.N., Eds.; Elsevier: Amsterdam, The Netherlands, 2020; pp. 499–535.
15. Yu, X.; Li, Y.; Gu, X.; Bao, J.; Yang, H.; Sun, L. Laser-induced breakdown spectroscopy application in environmental monitoring of water quality: A review. *Environ. Monit. Assess.* **2014**, *186*, 8969–8980. [CrossRef]
16. Bhatt, C.R.; Goueguel, C.L.; Jain, J.C.; McIntyre, D.L.; Singh, J.P. LIBS application to liquid samples. In *Laser-Induced Breakdown Spectroscopy*, 2nd ed.; Singh, J.P., Thakur, S.N., Eds.; Elsevier: Amsterdam, The Netherlands, 2020; pp. 231–245.
17. Lazic, V.; Jovićević, S. Laser induced breakdown spectroscopy inside liquids: Processes and analytical aspects. *Spectrochim. Acta Part B At. Spectrosc.* **2014**, *101*, 288–311. [CrossRef]
18. Keerthi, K.; George, S.D.; Kulkarni, S.D.; Chidangil, S.; Unnikrishnan, V. Elemental analysis of liquid samples by laser induced breakdown spectroscopy (LIBS): Challenges and potential experimental strategies. *Opt. Laser Technol.* **2022**, *147*, 107622. [CrossRef]
19. Fichet, P.; Mauchien, P.; Wagner, J.-F.; Moulin, C. Quantitative elemental determination in water and oil by laser induced breakdown spectroscopy. *Anal. Chim. Acta* **2001**, *429*, 269–278. [CrossRef]

20. Sobral, H.; Sanginés, R.; Trujillo-Vázquez, A. Detection of trace elements in ice and water by laser-induced breakdown spectroscopy. *Spectrochim. Acta Part B At. Spectrosc.* **2012**, *78*, 62–66. [CrossRef]
21. Knopp, R.; Scherbaum, F.J.; Kim, J.I. Laser induced breakdown spectroscopy (LIBS) as an analytical tool for the detection of metal ions in aqueous solutions. *Anal. Bioanal. Chem.* **1996**, *355*, 16–20. [CrossRef] [PubMed]
22. Chang, R.K.; Eickmans, J.H.; Hsieh, W.-F.; Wood, C.F.; Zhang, J.-Z.; Zheng, J.-B. Laser-induced breakdown in large transparent water droplets. *Appl. Opt.* **1988**, *27*, 2377–2385. [CrossRef] [PubMed]
23. Lui, S.L.; Godwal, Y.; Taschuk, M.T.; Tsui, Y.Y.; Fedosejevs, R. Detection of Lead in Water Using Laser-Induced Breakdown Spectroscopy and Laser-Induced Fluorescence. *Anal. Chem.* **2008**, *80*, 1995–2000. [CrossRef] [PubMed]
24. Cheri, M.S.; Tavassoli, S.H. Quantitative analysis of toxic metals lead and cadmium in water jet by laser-induced breakdown spectroscopy. *Appl. Opt.* **2011**, *50*, 1227–1233. [CrossRef]
25. Hahn, D.W.; Carranza, J.E.; Arsenault, G.R.; Johnsen, H.A.; Hencken, K.R. Aerosol generation system for development and calibration of laser-induced breakdown spectroscopy instrumentation. *Rev. Sci. Instrum.* **2001**, *72*, 3706–3713. [CrossRef]
26. Diaz, D.; Hahn, D.W. Aerosol measurements with laser-induced breakdown spectroscopy and conditional analysis. *Spectrochim. Acta Part B At. Spectrosc.* **2021**, *179*, 106107. [CrossRef]
27. Radziemski, L.J.; Loree, T.R.; Cremers, D.A.; Hoffman, N.M. Time-resolved laser-induced breakdown spectrometry of aerosols. *Anal. Chem.* **1983**, *55*, 1246–1252. [CrossRef]
28. Senesi, G.; Dell'aglio, M.; Gaudiuso, R.; De Giacomo, A.; Zaccone, C.; De Pascale, O.; Miano, T.; Capitelli, M. Heavy metal concentrations in soils as determined by laser-induced breakdown spectroscopy (LIBS), with special emphasis on chromium. *Environ. Res.* **2009**, *109*, 413–420. [CrossRef]
29. Goncharova, I.; Guichaoua, D.; Taboukhat, S.; Tarbi, A.; Chtouki, T.; Erguig, H.; Sahraoui, B. Laser-induced breakdown spectroscopy application for heavy metals detection in water: A review. *Spectrochim. Acta Part B At. Spectrosc.* **2024**, *217*, 106943. [CrossRef]
30. Buckley, S.G.; Johnsen, H.A.; Hencken, K.R.; Hahn, D.W. Implementation of laser-induced breakdown spectroscopy as a continuous emissions monitor for toxic metals. *Waste Manag.* **2000**, *20*, 455–462. [CrossRef]
31. Panne, U.; Neuhauser, R.; Theisen, M.; Fink, H.; Niessner, R. Analysis of heavy metal aerosols on filters by laser-induced plasma spectroscopy. *Spectrochim. Acta Part B At. Spectrosc.* **2001**, *56*, 839–850. [CrossRef]
32. Hahn, D.W.; Flower, W.L.; Hencken, K.R. Discrete Particle Detection and Metal Emissions Monitoring Using Laser-Induced Breakdown Spectroscopy. *Appl. Spectrosc.* **1997**, *51*, 1836–1844. [CrossRef]
33. Lee, Y.; Oh, S.-W.; Han, S.-H. Laser-Induced Breakdown Spectroscopy (LIBS) of Heavy Metal Ions at the Sub-Parts per Million Level in Water. *Appl. Spectrosc.* **2012**, *66*, 1385–1396. [CrossRef] [PubMed]
34. Zhao, F.; Chen, Z.; Zhang, F.; Li, R.; Zhou, J. Ultra-sensitive detection of heavy metal ions in tap water by laser-induced breakdown spectroscopy with the assistance of electrical-deposition. *Anal. Methods* **2010**, *2*, 408–414. [CrossRef]
35. Aras, N.; Yeşiller, S.Ü.; Ateş, D.A.; Yalçın, Ş. Ultrasonic nebulization-sample introduction system for quantitative analysis of liquid samples by laser-induced breakdown spectroscopy. *Spectrochim. Acta Part B At. Spectrosc.* **2012**, *74–75*, 87–94. [CrossRef]
36. Palazzo, N.; Migliorini, F.; Dondè, R.; Maffi, S.; De Iuliis, S. Influence of oxygen addition to the carrier gas on laser-induced breakdown spectroscopy measurements on aerosols. *Spectrochim. Acta Part B At. Spectrosc.* **2016**, *115*, 1–7. [CrossRef]
37. Redoglio, D.A.; Palazzo, N.; Migliorini, F.; Dondè, R.; De Iuliis, S. Laser-Induced Breakdown Spectroscopy Analysis of Lead Aerosol in Nitrogen and Air Atmosphere. *Appl. Spectrosc.* **2017**, *72*, 584–590. [CrossRef]
38. Long, G.; Winefordner, J.D. Detection limit: A closer look at IUPAC defination. *Anal. Chem.* **1983**, *55*, 712–724.
39. Hess, D.R. Nebulizers: Principles and performance. *Respir. Care* **2000**, *45*, 609–622.
40. Dennis, J.H.; Hendrick, D.J. Design characteristics for drug nebulizers. *J. Med. Eng. Technol.* **1992**, *16*, 63–68. [CrossRef] [PubMed]
41. Turns, S. *An Introduction to Combustion—Concepts and Applications*; McGraw-Hill Inc.: New York, NY, USA, 1996.
42. Kramida, A.; Ralchenko, Y. *NIST Atomic Spectra Database (Ver. 5.11)*; National Institute of Standards and Technology: Gaithersburg, MD, USA, 2021. [CrossRef]
43. Fortes, F.J.; Moros, J.; Lucena, P.; Cabalín, L.M.; Laserna, J.J. Laserna, Laser-Induced Breakdown Spectroscopy. *Anal. Chem.* **2013**, *85*, 640–669. [CrossRef] [PubMed]
44. Cremers, D.; Radziemski, L. Qualitative LIBS analysis. In *Handbook of Laser-Induced Breakdown Spectroscopy*, 2nd ed.; Wiley: Chichester, UK, 2013; pp. 151–159.
45. Mohamed, W.T.Y. Improved LIBS limit of detection of Be, Mg, Si, Mn, Fe and Cu in aluminum alloy samples using a portable Echelle spectrometer with ICCD camera. *Opt. Laser Technol.* **2008**, *40*, 30–38. [CrossRef]
46. Syvilay, D.; Guezenoc, J.; Bousquet, B. Guideline for increasing the analysis quality in laser-induced breakdown spectroscopy. *Spectrochim. Acta Part B At. Spectrosc.* **2019**, *161*, 105696. [CrossRef]
47. Diaz, D.; Hahn, D.W. Plasma chemistry produced during laser ablation of graphite in air, argon, helium and nitrogen. *Spectrochim. Acta Part B At. Spectrosc.* **2020**, *166*, 105800. [CrossRef]

Disclaimer/Publisher's Note: The statements, opinions and data contained in all publications are solely those of the individual author(s) and contributor(s) and not of MDPI and/or the editor(s). MDPI and/or the editor(s) disclaim responsibility for any injury to people or property resulting from any ideas, methods, instructions or products referred to in the content.